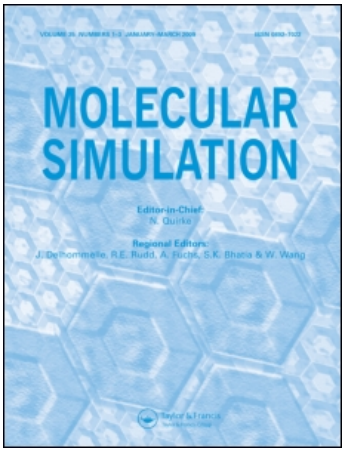

Molecular Simulation
Publication details, including instructions for authors and subscription information:
http://www.informaworld.com/smpp/title~content=t713644482

Predicting the Rheology of Complex Fluids

Leslie V. Woodcock[a]
[a] Schools of Chemical Engineering, University of Bradford, Bradford, West Yorkshire, U.K.

To cite this Article Woodcock, Leslie V.(1989) 'Predicting the Rheology of Complex Fluids', Molecular Simulation, 2: 4, 253 — 279
To link to this Article: DOI: 10.1080/08927028908034605
URL: http://dx.doi.org/10.1080/08927028908034605

Molecular Simulation, 1989, Vol. 2, pp. 253–279
Reprints available directly from the publisher
Photocopying permitted by license only

PREDICTING THE RHEOLOGY OF COMPLEX FLUIDS†

LESLIE V. WOODCOCK

Schools of Chemical Engineering, University of Bradford, Bradford BD7 1DP, West Yorkshire, U.K.

(*Received May, 1988; in final form July, 1988*)

Progress towards the absolute prediction of the constitutive rheological relations of more complex fluids using the methods of non-equilibrium molecular/particulate dynamics simulations is reviewed. The approaches are based upon the initial use of simple hard–, soft–, and colloidal-sphere effective pair potentials and corresponding state scaling analyses. The general objective is illustrated initially using results for the soft-sphere fluid viscosity, and soft-sphere scaling laws to predict the Newtonian viscosities of simple molecular liquids and gases for physical data banks. It is further shown how the non-Newtonian behaviour of these simple hard– and soft-sphere models can be scaled to predict the flow curves of colloidal suspensions when the models and equations-of-motion are appropriately modified or scaled to take account of the mean hydrodynamic flow field, solvation and/or Brownian motion effects of the medium.

Preliminary extensions towards the prediction of dry powder flow using methods of granular dynamics are also reported: the collisional dynamics are damped by an effective coefficient of restitution which leads to similar scaling laws; gravitational scaling units may also be used in this case.

KEY WORDS: Rheology, complex fluids, non-equilibrium molecular dynamics, soft-spheres, scaling laws.

1. INTRODUCTION

Fluid flow can often be predicted, and hence understood, within the framework of continuum hydrodynamics (given material constants) when some or all of the difficulties associated with coupled phenomena of compressibility, bulk and elongational viscosity, heat capacity, thermal conductivity, entropy production, gravity, turbulence are negligible. Both the material constant concept, and the continuum approximation break down for processes where the perturbation distance scale is of the order of particulate force correlations, where the time-scale is of the order of particulate stress correlations, or where the amplitude of shear gradient is sufficient to distort the local thermodynamic equilibria. Such are the circumstances for all non-Newtonian viscous responses of complex fluids; examples include concentrated dispersions, polymer melts, many emulsions, glass-forming liquids, all solids (finite shear modulus at zero frequency) and granular materials; hence the need for particulate simulations to establish the origins of the constitutive rheology [1].

The molecular transport theory of Newtonian fluids, likewise, can only be expected to proceed to fruition by neglecting troublesome terms in the molecular Hamiltonian that are not significantly manifested in the macroscopic phenomena. For the shear viscosity of a liquid, when complexities arising from non-pairwise additivity, long-range potentials, intramolecular degrees-of-freedom and quantum effects are all discounted, little may b e lost from the interpretive or predictive ability of the residual models from the standpoint of the theoretical physicist or the chemical engineer.

Whatever the application, experience tells us that 'the more one tries to put into a

†Invited paper.

simulation, the less one gets out'. Corresponding states scaling laws for the effective hard- and soft-sphere model pair potentials indicate that, whilst analytic theories are still lacking, the quantitative values for the shear viscosities of simple fluids may be predicted at least up to the uncertainty with which they can presently be measured. The design engineer rarely requires 3-figure accuracy but he must avoid catastrophe or gross misdesign.

Since the discovery of exact relationships between non-equilibrium fluxes of mass, momentum and energy, and equilibrium fluctuations of velocity, stress and heat flow, respectively [2], numerical molecular dynamics (MD) computations [3] have been used to derive the appropriate correlation functions leading to the determination of shear viscosity coefficients for simple model fluids of hard- and soft-spheres [4,5]. Motivated initially by the computational tedience of accurate correlation function computations, heuristic techniques of non-equilibrium molecular dynamics (NEMD) were developed [6–9]. In these steady-state MD methods external work is performed on the system and arbitrary thermostatting is applied. Phenomenological hydrodynamics is implicit in relating the resulting momentum fluxes to linear transport coefficients. The main advantage of NEMD, however, is that it can be used to obtain non-linear transport coefficients that cannot be calculated in any other way.

The NEMD computations are less costly than determining fluctuation correlations, but suffer from the uncertainty of extrapolating to the small gradient limit of hydrodynamics. Whilst fluctuation theory may be the appropriate technique for the linear transport coefficients and their frequency spectra, the NEMD methods have a wide scope for predicting the technologically important aspects of non-Newtonian flow for complex fluids including colloidal suspensions and powders. Indeed, as a consequence of the coupling complications mentioned above, these computations do not relate to non-Newtonian behaviour of simple liquids although all fluids would be non-Newtonian at sufficient shear rates; at the ultra high shear rates at which simple liquids or gases become non-Newtonian the thermal gradients would be dominant. The description non-Newtonian is used in a broad sense for any fluid whose apparent viscosity from rheometric measurement is found to be shear rate dependent.

NEMD computations, nevertheless, at strongly non-Newtonian shear rates have shown that these simple repulsive models, without many-body hydrodynamics or Brownian motion effects, can exhibit all the common non-Newtonian flow phenomena observed in dense suspensions such as shear dilatancy and shear thickening phenomena [10] and thixotropy [11]. Up to now absolute quantitative predictions for the apparent viscosity of these complex materials have not been made, although we do have a much better understanding of the gneral phenomenology and experimental difficulties [12].

In the following sections it will be described how these computations may in the foreseeable future be used to make quantitative predictions of dense colloidal suspensions and granular materials under shear flow. After a discussion on effective pair potentials, the approach will be introduced and illustrated by first demonstrating the use of soft-sphere scaling variables to predict the viscosities of simple atomic and molecular fluids following the original observations of Ashurst and Hoover regarding the potential usefulness of scaling laws for data predictions [13].

2. EFFECTIVE PAIR POTENTIALS

Owing to the complexity of interparticle forces, for all fluids from liquid argon to

colloidal suspensions, an essential concept is the effective pair potential. This determines the total interaction force on a particle by

$$F_i(t) = \sum_{j \neq i} - \frac{d\phi_{eff}}{dr_{ij}}(r_{ij}) ; \quad (1)$$

given the equation-of-motion and the requisite prescribed state variables, volume and temerature, it determines a unique set of bulk properties, for the model material which it defines, when two independent state variables are fixed, e.g. V and T.

In general, an effective pair potential would be both state–, and property-dependent, to be truly effective over the whole range of V,T and physical properties; it may differ substantially from the so-called "true" pair potential of two particles in isolation. The thermodynamic and transport properties of many molecular liquids and gases are now known to be well-represented by the Lennard-Jones pair potential [14].

$$\phi_{ij} = 4\varepsilon_{LJ}\left\{\left(\frac{\sigma}{r}\right)^{12} - \left(\frac{\sigma}{r}\right)^{6}\right\} \quad (2)$$

Our understanding of the properties of simple liquids has developed in the gradual realisation that predominant liquid-state thermodynamic and transport properties are all primarily determined by the repulsive part of the effective pair potential. Bulk properties relate to average local structures, and fluctuations in local structures for transport properties, which are largely determined by interparticle repulsions.

Essential properties of an effective pair potential for predictive purposes, therefore, are simplicity and scalability. The soft-sphere model represents only the repulsive part of the Lennard-Jones potential (for n = 12)

$$\phi(r) = \varepsilon_{ss}\left(\frac{\sigma}{r_{ij}}\right)^{n} \quad (3)$$

and corresponds to the hard-sphere model when n goes to infinity. A single hybrid state variable defines the state of the soft-sphere model because changes in reduced temperature (kT/ε_{ss}) are equivalent to changes in the reduced volume ($V/N\sigma^3$) by the linear scaling of $\varepsilon_{ss}\sigma^{n/3}$.

The physical laws that derive from this unique scaling provide a basis for predicting the viscosity of simple liquids [8] and a starting point for understanding dense suspensions [10,11]. The general requirement is that the viscosity is primarily determined by the scaling variables of particulate mass, size and energy, and corresponds to a scaleable model of known properties from computer simulations. Complexities such as interparticle attractions or non-spherical potentials, can then be regarded as perturbations.

The essential question arising with complex materials such as colloidal suspensions concerns what determines the essential physics of their properties, e.g. the rheology, and what constitutes the perturbation. An effective pair potential for the interaction between colloidal spheres in lyophobic (aqueous) media was derived by Verwey and Overbeek in 1948 [15] using classical electrostatics and based partly on theory previously developed by Derjaguin and Landau. This theoretical effective pair potential (known as DLVO) has remained virtually intact, but still largely untested, as the accepted description of the behaviour of lyophobic colloids for 40 years. It is not suitable for predictive simulation studies of suspension rheology however, because it contains too many empirical parameters and it is not amenable to scaling. Moreover, it is inapplicable to lyophillic-type colloids and the attractive term in the effective pair

potential, ascribed only to dispersion forces, may not represent the essential physics because it neglects the bulk thermodynamics arising from solvation effets which may well be dominant.

Difficulties with the short-range solvation at high packing and the 'screened coulomb' forces, as well as representation of the inevitable polydispersity, can be accommodated into a generalisation of the hard– and soft–sphere models, and may be termed "colloidal spheres", when the effective pair potential takes the simple form

$$\phi_{ij} = \varepsilon_{cs}\left(\frac{r}{\sigma_{ij}} - 1\right)^{-n}; \tag{4}$$

the hard-sphere model is approached in the limits $n \to \infty$ and/or $\varepsilon \to 0$, and the soft-sphere scaling is recovered when $\sigma \to 0$, i.e. all $r_{ij} \gg \sigma$. Unlike the soft-sphere limit (equation 3), however, two state variables are generally required to specify the thermodynamic state of a system of colloidal soft-spheres. Equation (4) can represent the DLVO-type repulsion for smaller values of n; it is more appropriate for incorporating explicitly into the simulations the effects of polydispersity, i.e. a distribution of σ_{ij} and it can represent elastic repulsions arising from solvation effects. It is also amenable to the inclusion of a restitution coefficient for the study of granular flow (section 7). Some preliminary thermodynamic equations-of-state data for n = 12 colloidal spheres which could be fitted to osmotic pressure data are given in Appendix I.

The need for soft-repulsions between fine particles in dense suspension becomes evident when we consider the average distance between neighbouring spheres in a typical monodisperse suspension of submicron spherical particles.

Consider the hard-sphere model. The osmotic equation-of-state is given by

$$\frac{pV}{NkT} = 1 + \frac{2}{3}\pi\rho g(\sigma) \tag{5}$$

where ρ is $N\sigma^3/V$ and $g(\sigma)$ is the pair distribution function at contact. To obtain $g(\sigma)$ we can use a simple but very accurate self-consistent free volume equation-of-state for the hard-sphere fluid up to amorphous random close-packing [16]

$$\frac{pV}{NkT} = \left[1 - \left(\frac{V_o}{V}\right)^{1/3}\right] \tag{6}$$

where V_o is the maximum *amorphous* close-packed volume per particle corresponding to the packing fraction y = 0.6366 (or $\sim 2/\pi$). The average number of neighbours up to a short distance x from a sphere is

$$n(x) = \int_{\sigma}^{\sigma+x} 4\pi r^2 \rho g(\sigma)\, dr \tag{7}$$

Substituting for $g(\sigma)$ from equations (5) and (6), putting n = 1, and solving for x we obtain an accurate estimate of the average distance to the first neighbour for a hard-sphere suspension

$$x = \left[\frac{1}{3\pi y} + \frac{5}{6}\right]^{1/2} - 1 \tag{8}$$

This simple result, plotted in Figure 1, shows that even when the packing fraction y is 0.5, the average distance between first neighbours is $\sigma/100$. Recent experimental

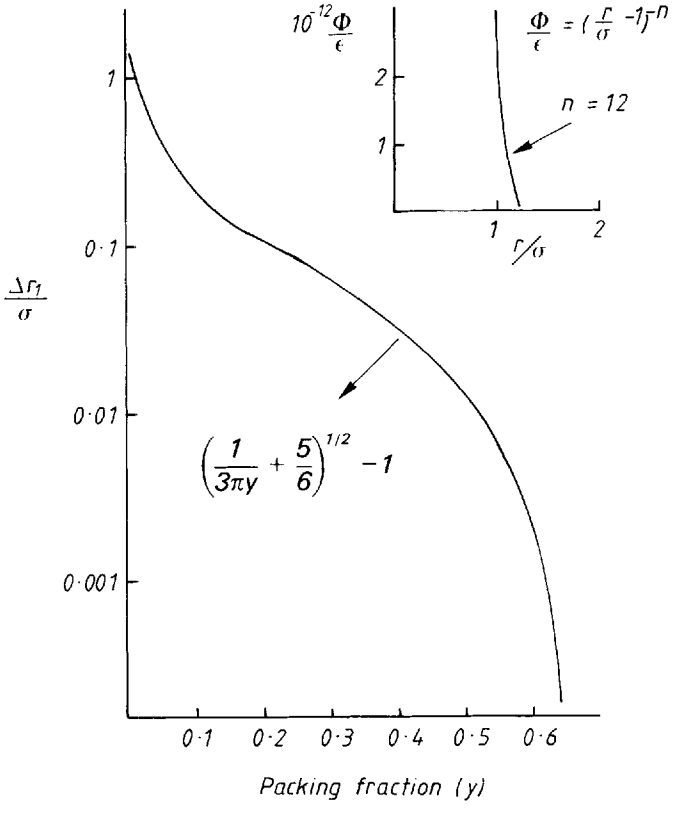

Figure 1 A plot of the average surface-to-surface distance to the first near neighbour against packing fraction for the hard-sphere fluid at equilibrium, metastable equilibrium and glassy states up to amorphous random close packing; $\Delta r_1/\sigma$ is the mean separation ($r_{ij}/\sigma - 1$); the plot represents equation (8) derived in the text; the inset shows the colloidal-sphere potential (equation (4)) (n = 12) for representing solvation and/or lubrication effects.

studies of hard-sphere suspensions have been reported for silica shperes ($\sigma \sim 0.2$ nm) in cyclohexane [17]; in this case, for example, the distance is about 1 solvent molecule diameter at 50% packing! Since there are possible surface ordering effects, and surface roughness of molecular magnitudes, we do not expect long-range many-body hydrodynamic effects, or Brownian motion, to be relevant for these systems in the intermediate to high packing range.

The predominant force on a colloidal particle in dense suspension derives from near-neighbour collisional or geometric effects which may be accommodated into the colloidal sphere potential, equation (4), by approximately parametrising the values of ε and n as shown in the inset to Figure 1. The characteristic energy ε needs to be expressed in terms of a modified friction constant to take account of the elastic effects of solvation with a degree of inelasticity in the form of a coefficient of restitution for the wide range of behaviour from purely hydrodynamic to granular-like flow.

3. MOLECULAR FLUIDS

In 1975, Ashurst and Hoover reported NEMD computations of the Newtonian viscosities of both the Lennard-Jones and soft-sphere (n = 12) models [8,13]. They found that the soft-sphere fluid viscosity over the whole range from dilute gas to freezing transition is well-represented by a very simple expression in terms of the reduced variables ($V^{*4}T^*$ is the hybrid independent state variable).

$$\eta^*_S = T^{*2/3}\left(a + \frac{b}{V^{*4}T^*}\right) \tag{9}$$

where the asterisks denote the reduced quantities

$$\eta^*_S = \frac{\eta\sigma^2}{(m\varepsilon)^{1/2}}; V^* = \frac{V}{N\sigma^3}; T^* = \frac{kT}{\varepsilon}$$

The density-independent contribution $aT^{*2/3}$ is the low pressure limit of the gas viscosity from kinetic theory. For soft-spheres the constants in equation (9) are $a = 0.171$ and b was found to be 3.025.

Ashurst and Hoover noted two properties of this expression which agree with real experimental observations of fluid viscosity data:

(i) a quantitative similarity between the Lennard-Jones fluid viscosity η^*_{LJ} and that predicted from η^*_{ss} (when the correction for $\varepsilon_{ss} \equiv 4\varepsilon_{LJ}$ is made to the scaling), both in line with experimental data for argon down to low temperatures, and

(ii) a weak temperature dependence of viscosity with a negative temperature derivative of the excess part of the viscosity ($\eta^* - aT^{*2/3}$) at constant density.

The viscosity of gases increases with temperature whereas the viscosity of liquids decreases with temperature. The simple explanation of these observations advanced by Ashurst and Hoover [8] is seen very clearly in the soft-sphere scaling laws but had not previously been attributed to the dominance of an effective repulsive pair potential.

The temperature derivative of equation (9)

$$\frac{d\eta^*}{dT} = \frac{2}{3}aT^{*-1/3} - \frac{1}{3}bV^{*-4}T^{*-4/3} \tag{10}$$

shows the dominance of the excess part when V* is small.

η^*_{LJ} calculated directly from NEMD and η^*_{LJ} predicted from equation (9) would be identical if the viscosity depend entirely and only upon the repulsive term in the Lennard-Jones pair potential at the same V^*, T^* state point. The reduced excess shear viscosity from soft-spheres, however, predicts the Lennard-Jones and liquid argon viscosities very well in the range $(V^{*4}T^*)^{1/4} > 0.5$ (i.e. in the supercritical range) but, over the whole range, it was found that a better fit could be obtained using a slightly more complicated 2-parameter expression for the excess part;

$$\text{from } \eta^*_S: \eta^*_{LJ} = T^{*2/3}\left[c + 0.0152\left\{\exp\left(\frac{7.02}{T^{*1/4}V^*}\right) - 1\right\}\right] \tag{11}$$

$$\text{from NEMD}_{LJ}: \eta^*_{LJ} = T^{*2/3}\left[c + 0.0240\left\{\exp\left(\frac{6.0}{T^{*1/4}V^*}\right) - 1\right\}\right] \tag{12}$$

where the constant c represents the kinetic theory result for the low pressure gas viscosity from the collision integral cross section for the Lennard-Jones pair potential (c is calculated to be 0.1357). These equations differ mainly in the predicted viscosity at high temperature. Ashurst and Hoover finally, therefore, used a computer curve fit to obtain the best hybrid equation to parametrise both the Lennard-Jones and the soft-sphere results

$$\eta^*_{LJ} = T^{*2/3}\left[c + a\left(1 - \frac{1}{2T^{*1/2}} + \frac{2}{T^*}\right)\exp\left\{\frac{b}{V^*T^{*1/4}}\left[1 - \frac{5}{T^{*1/2}}\right]\right\} - 1\right] \tag{13}$$

where a = 0.0152; b = 7.02 and c = 0.1357.

The 'fit error' in obtaining this hybrid expression is everywhere less than 10% of the dilute gas shear viscosity. It was found to reproduce hydrogen and deuterium excess shear viscosity data up to 2000 atmospheres to within 2% and data on liquid argon to within 5%.

Using tabulated values of effective Lennard-Jones parameters from various sources, we have tested the predictive ability of this soft-sphere scaling equation for a number of more complex molecular liquids [18]. The tests cover a wide range of V^*, T^* state points, from the triple point to the dilute gas, initially taking the ε, σ molecular parameters directly from the original gas viscosity data tabulations [19]. From a data prediction-storage-retrieval standpoint the results are remarkably encouraging. Figure 2, taken from reference [18], shows the most severe test, highly non-spherical molecules, using gas-viscosity [19] ε, σ values, and comparing along the liquid coexistence line. The worst deviations are no more than 50% of the experimental data over the whole range of comparisons spanning many orders-of-magnitude of viscosity.

The discrepancies in Figure 2, moreover, were found to arise not primarily from an inherent inadequacy of equation (13), in representing complex molecules, but more in

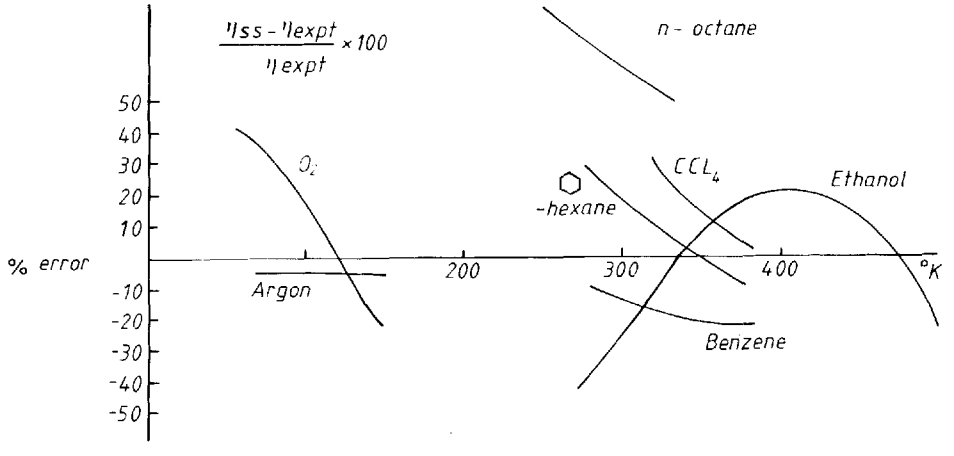

Figure 2 Discrepancies between soft-sphere scaling law predictions and experimental values for the shear viscosities of a range of molecular liquids at states along the liquid-vapour coexistence line; these margins of error are substantially reduced when the molecular parameters ε or σ are fitted to the U(V,T) and p(V,T) equations-of-state for the state points predicted (reproduced from reference [18]).

the failure of the raw ε, σ parameters from low density gas origins to get the equation-of-state p^* (V^*, T^*) right at low temperatures and pressures. When effective values of ε, σ are used which exactly fit the equations-of-state U^* (p^*, T^*) and V^* (p*, T^*) respectively, at the same state point of comparison, the predictive ability of the soft-sphere scaling equations are of the order $< 10\%$ for the range of liquids shown in Figure 2.

We can now work towards obtaining better effective ε and σ values, by optimising over the whole range, and also towards the incorporation of perturbations for dipolar and accentric factors from readily available molecular constants for more complex molecules. It is worth noting, in passing, that similar scaling prediction of molecular fluid thermal conductivities has produced more promising results than the viscosity predictions because the thermal conductivity is less sensitive to the choice of the effective σ parameter than the viscosity [13, 20] but similarly dominated by the repulsive pair potential.

4. MEAN FIELD STOKESIAN DYNAMICS

The extension of particulate simulation techniques to the strongly non-Newtonian flow domain is now well established [21, 22]; a diversity of characteristic flow phenomena for dense colloidal suspensions has been shown to occur in simple effective-repulsion soft-sphere models. Shear thinning, thickening, dilatancy and anisotropic effects can be described as a shear perturbation of the equilibrium osmotic behaviour. Sheared-phase behaviour such as the ordering and disordering transitions is determined originally by the static phase boundaries and, for hard-spheres, maximum packing singularities [21] (see Appendix II).

Most of the NEMD computations that relate to suspensions have been isokinetic, i.e. the total kinetic energy of the particles is held fixed by scaling the peculiar velocities of the particles (i.e. relative to the flow field) using either continuous renormalisation or modified equations-of-motion to effect the same results [23]. Up to now absolute prediction of the constitutive rheology of suspended particles has not been possible because, in real laboratory experiments, the particulate kinetic energies are a dependent variable of the medium characteristics and the rate of shear flow.

Extending the computer simulation methodology, we have developed programs for the *ab initio* calculation of the flow curves (pressure tensor as a function of shear rate) for the idealised hard-core models in a Newtonian medium of prescribed viscosity. The medium viscosity is incorporated into the many-particle dynamics algorithm in the form of a mean Stokes friction constant; since multi-body hydrodynamic interactions are explicitly omitted the method may be referred to as mean-field Stokesian dynamics [24].

The equations-of-motion take the form

$$d\mathbf{r}_i = \mathbf{v}_i dt \tag{14}$$

$$d\mathbf{v}_i = \frac{1}{m}(\mathbf{F}_i^{(H)} + \mathbf{F}_i^{(P)})\, dt \tag{15}$$

where $\mathbf{F}_i^{(H)}$ and $\mathbf{F}_i^{(P)}$ are the hydrodynamic and interparticulate forces respectively. $\mathbf{F}_i^{(P)}$ is given as in equation (1) from the effective pair potentials and

$$\mathbf{F}_i^{(H)} = -\mathbf{v}_i \mathbf{S}_i + \sum_{j \neq i} \mathbf{S}_{ij} \cdot \mathbf{F}_j^{(H)}\,; \tag{16}$$

the second term is the many-body hydrodynamics and S_{ij} is the effective two-body friction tensor and S_i the Stokes friction force is $3\pi\sigma\eta_m$.

Neglecting the many-body terms we can consider the equations-of-motion of N-Stokesian hard-spheres. In this case the Stokes friction constant determines the scaling; the equations-of-motion between collisions are

$$\frac{d^2\mathbf{r}_i}{dt^2} = -C\frac{d\mathbf{r}_i}{dt} \tag{17}$$

where $C = 3\pi\sigma\eta_m/m$ and C^{-1} sets the time scale. Integration gives the expressions for the positions and velocities

$$\mathbf{r}_i(t) = \mathbf{r}_i(0) + \mathbf{v}_i(0)\left(\frac{1 - \exp(-Ct)}{C}\right) \tag{18}$$

$$\mathbf{v}_i(t) = \mathbf{v}_i(0)\exp(-Ct) \tag{19}$$

On expanding the exponential and taking the limit $C \to 0$ Newtonian dynamics are recovered. The time to the 'next collision' between any two spheres can be obtained from the quadratic (see Appendix III)

$$r_{ij}(0) - \sigma^2 + 2\mathbf{r}_{ij}(0)\,\mathbf{v}_{ij}(0)\left(\frac{1 - \exp(-Ct)}{C}\right) + \mathbf{v}_{ij}^2(0)\left(\frac{1 - \exp(-Ct)}{C}\right)^2 = 0 \tag{20}$$

By putting

$$x = \frac{1 - \exp(-Ct)}{C} \tag{21}$$

we can proceed, as with Newtonian spheres, obtaining x from the positive real root of the general quadratic, to give the collision time from

$$\Delta t = -\frac{1}{C}\ln(1 - Cx) \tag{22}$$

The collisions obey reversible classical mechanics conserving total momentum; a restitution coefficient could be incorporated for inelastic collisions (see section 7).

At every collision in a hard-sphere Stokesian simulation all the particle positions and velocities are recalculated according to the equations-of-motion (18) and (19). In this simple scheme, for hard spheres, the flow-field velocity may only be influential at the driving boundaries. When a constant Y-dependent component of v_i^x is imposed for homogeneous shear the quadratic equation (20) becomes a quartic, which is, however, still amenable to computational solution (Appendix III). The osmotic pressure tensor is computed, as in Newtonian dynamics, by taking the time-average of the momentum transferred over all the collisions.

The time-scaling relationship implied by equations (21) and (22) between Newtonian isokinetic dynamics and mean-field Stokesian dynamics shows that the two systems have identical dynamical properties for large N. The Stokesian dynamics for unperturbed spheres gives exactly the same configurational trajectories as the classical hard-sphere fluid at equilibrium but with an ever-lengthening time scale. For non-equilibrium steady-state NEMD, in the limit of a sufficiently high scaling frequency

in the damped Newtonjian dynamics, every collision or time-step, all ensemble time-averages of the two methods become mutually predictable.

In continuous effective pair potential simulations, for example soft-spheres or the colloidal-sphere potential in Figure 1, momentum renormalisation at every time-step effects a similar correspondence to mean-field Stokesian dynamics. Whereas in previous damped Newtonian NEMD computations the total kinetic energy of the particles is held constant and the friction coefficient varies, in mean-field Stokesian dynamics the reduced friction coefficient ($C/\dot{\gamma}$) is the constant of the computation and the kinetic energy is free to fluctuate. In both cases the kinetic energy fluctuates between the Cartesian dimensions and a high degree of anisotropy develops at strongly non-Newtonian shear rates.

5. SCALING LAWS

The corresponding states scaling laws for the hard-sphere model in both isokinetic and Stokesian form are given in Table 1. It should be noted that in this section the superscript asterisk (*) is used to denote Stokesian-reduced properties and the superscript dagger (†) is used to denote isokinetic-reduced quantities.

For a system of spheres in steady-state quasiequilibrium at a given packing fraction (φ) the reduced bulk properties in either scheme are functions only of the appropriately reduced shear rate and the packing fraction. Thus, for the constitutive rheology we can write the stress tensor flow curves

Table 1 Definitions of reduced properties in the isokinetic and mean-field Stokesian suspensions together with the corresponding states scaling laws; the basic units are particle mass (m), diameter (σ), medium viscosity (η_m); the mean kinetic energy in the isokinetic scheme $E_0 = 1/2\, m\overline{v_i^2}$.

	Isokinetic	*Stokesian*[b]
time	$t^\dagger = t\left(\frac{E_0}{m\sigma^2}\right)^{1/2}$	$t* = tC$
shear rate	$\dot{\gamma}^\dagger = \dot{\gamma}\left(\frac{m\sigma^2}{E_0}\right)^{1/2}$	$\dot{\gamma}* = \dot{\gamma}/C$
friction coefficient	$C^\dagger = C\left(\frac{m\sigma^2}{E_0}\right)$	$\left(C = \frac{3\pi\sigma\eta_m}{m}\right)$
kinetic energy[a] (hydrodynamic "temperature")	$E^\dagger = E/E_0 = E*C^{*2}$	$E* = \frac{E}{m\sigma^2C^2} = \frac{E^\dagger}{C^{*2}}$
pressure (tensor)	$\mathbf{p}^\dagger = \mathbf{p}\,\sigma^3/E_0 = \frac{\mathbf{p}*}{E*}$	$\mathbf{p}* = \mathbf{p}\frac{\sigma}{mC^2} = \frac{\mathbf{p}^\dagger}{C^{*2}}$
viscosity	$\eta^\dagger = \eta\frac{\sigma^2}{(mE_0)^{1/2}} = \frac{\eta*}{E*^{1/2}}$	$\eta* = \frac{\eta}{3\pi\eta_m} = \frac{\eta^\dagger}{C^*}$
diffusivity	$D^\dagger = D\left(\sigma^2E_0\right) = \frac{D*}{E*^{1/2}}$	$D* = \frac{D}{C\sigma^2} = \frac{D^\dagger}{C^*}$

(a) For thermal systems E_0 is usually defined as kT (where k is Boltzmann's constant; T the absolute temperature) in this case $E^\dagger = \frac{3}{2}$ and the scaling relations require this factor to be included e.g. $p^\dagger = p*E^\dagger/E*$ etc.
(b) For the purpose of scaling the soft-sphere flow curve in figures (8) and (9) the kinetic energy E_0 is fixed equal to the constant ε in the soft-sphere pair potential.

$$\mathbf{p}^{\dagger}(\dot{\gamma}^{\dagger},y) \text{ and } \mathbf{p}^{*}(\dot{\gamma}^{*},y)$$

for isokinetic and Stokesian scaling respectively. To scale from isokinetic to Stokesian and/or vice versa Newtonian isokinetic dynamics or the mean kinetic energy in the Stokesian computation, i.e.

$$\langle C^{\dagger}(\dot{\gamma}^{\dagger}\, y)\rangle \text{ N,V,E or } \langle E^{*}(\dot{\gamma}^{*},y)\rangle \text{ N,V,C}$$

respectively. A consideration of the energy balance in isokinetic or thermalised calculations using NEMD for the Newtonian viscosity of the hard-sphere fluid enables predictions to be made of the Stokesian flow curve, and hence of experimental results for well-characterised suspensions where the hydrodynamic approximations may be valid.

In steady shear laminar flow the boundary-driven shearing force puts heat into the system according to

$$Q = \eta\dot{\gamma}^{2} \tag{23}$$

where Q is the power input per unit volume, η is the viscosity and $\dot{\gamma}$ the velocity gradient. In isokinetic simulationsthe total particle kinetic energy, defined as

$$E = \frac{m}{2}\sum_{i} v_{iy}^{2} + v_{iz}^{2} + (v_{ix} - v_{x}^{o}(y))^{2} \tag{24}$$

is held constant by scaling the peculiar velocities (i.e. the particle velocities relative to the flow field $v_x^o(y)$) according to the equations of motion [22, 24]

$$\left.\begin{aligned} d\mathbf{r}_i &= m\mathbf{v}_i\, dt \\ d\mathbf{v}_i &= \frac{\mathbf{F}_i}{m}\,dt + (f(t) - 1)m\mathbf{v}_i \\ f^{2}(t) &= \frac{3NkT_o}{m\sum_{i=1}^{N}\left(\mathbf{v}_i + \frac{\mathbf{F}_i}{m},\,dt\right)^{2}} \end{aligned}\right\} \tag{25}$$

or, in the case of Berendsen's isothermal heat bath [25]

$$\left.\begin{aligned} d\mathbf{v}_i &= \frac{\mathbf{F}_i}{m}\,dt + (f_B^{2}(t) - 1)m\mathbf{v}_i \\ f_B &= \frac{3NkT_o}{m\sum_{i=1}\mathbf{v}_i^{2}} \end{aligned}\right\} \tag{26}$$

In either case, in the limit $dt \to 0$, an energy balance for the steady-state homogeneous shear simulation gives

$$3NkT_o\ \langle f(t) - 1\rangle = \langle \eta\,\dot{\gamma}^{2}V\,dt\rangle \tag{27}$$

heat out heat in

where the brackets denote time averages. If a friction coefficient is defined as

$$C\,dt = f(t) - 1$$

we obtain the simple scaling result for the mean-field Stokesian friction coefficient when it is expressed in isokinetic H-S units.

$$C^{\dagger} = \frac{v^{\dagger}\dot{\gamma}^{\dagger 2}}{3\varrho^{\dagger}} \tag{29}$$

The Newtonian viscosity obtained from low $\dot{\gamma}^{\dagger}$-shear for the thermalised hard-sphere fluid can therefore be y) from equation-of-state data, and suspension rheology at high shear from the viscosity of the hard-sphere fluid. From the definition of E^* (Table 1)

$$E^*(\dot{\gamma}^*, y) = \frac{E^{\dagger}}{C^{\dagger 2}}\Bigg|_{\dot{\gamma}^{\dagger}, y} \tag{30}$$

and

$$\dot{\gamma}^* = \frac{\dot{\gamma}^{\dagger}}{C^{\dagger}} = \frac{3\varrho^{\dagger}}{\eta^{\dagger}C^{\dagger}} \tag{31}$$

For thermalised systems $E^{\dagger} = \frac{3}{2}$; for hydrodynamic systems we must introduce the concept of the "hydrodynamic temperature", E*, by analogy with the "granular temperature" often used in powder flow. The "hydrodynamic temperature" is a non-thermal concept, but it may embody contributions to the particle velocities from the thermal effects of Brownian motion (section 6).

To illustrate the possibilities for using scaling laws to make predictions about suspension rheology in general we refer to a recent review of experimental data for more than 100 suspensions by Barnes [26]. It was found that the characteristic shear rate that marks the onset of shear thickening correlates with the particle size squared (Figure 1). In Stokesian scaling the reduced characteristic shear rate is the dimensionless group ($\rho = Nm/V$)

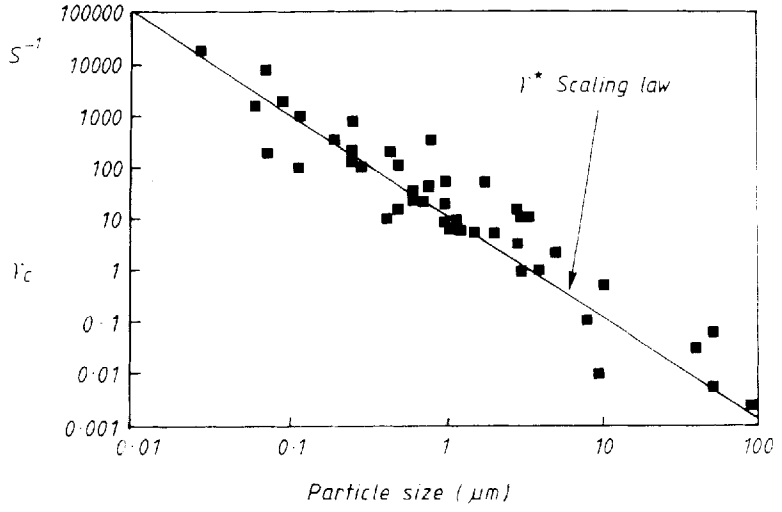

Figure 3 A collection of literature data for the critical characteristic shear rate at the onset of shear thickening as a function of mean particle size from an analysis of more than 100 experimental systems by H.A. Barnes (reference [26]): the straight line corresponds to the $\dot{\gamma}^*$-scaling law.

$$\dot{\gamma}^* = \frac{4}{9}\frac{\sigma^2\dot{\gamma}\rho}{\eta_m} \tag{32}$$

Figure 3 illustrates the general obedience of flow-curve data to the $\dot{\gamma}^*$-scaling law. Apart from the constant, this dimensionless ratio has long been recognised empirically as a determining characteristic group for suspension rheology [27].

Calculations for the hard-sphere model flow curves using both NEMD and Stokesian schemes are in progress but at present we do not have sufficient data over the whole flow curve non-Newtonian range to demonstrate the scaling. The soft-sphere data [21], however, are equally amenable to scaling and the effect of the scaling on the kinetic energies is shown in Figure 4. The damped Newtonian kinetic energy at non-Newtonian shear-rates shows large normal differences, which are manifested

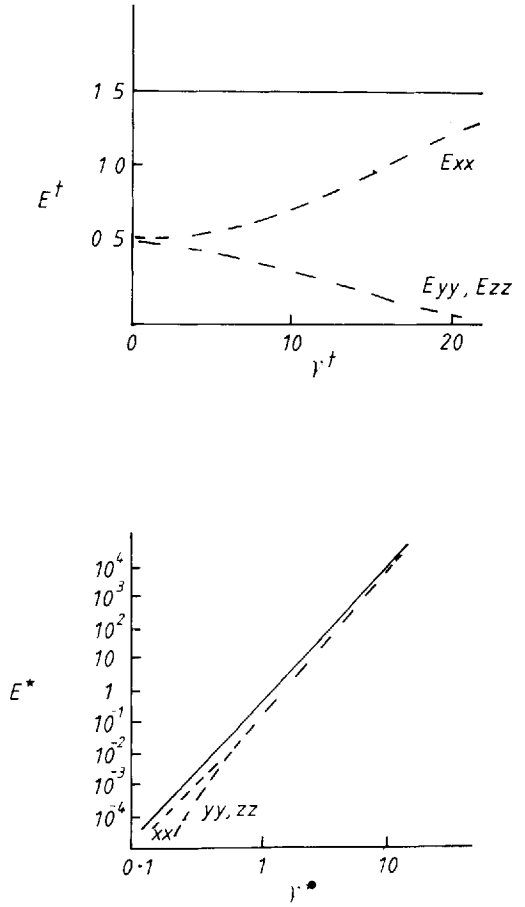

Figure 4 A comparison of the reduced kinetic energies in isokinetic and mean-field Stokesian dynamics simulations; at non-Newtonian shear rates the isokinetic $E^\dagger$, in units of kT, shows increasingly large normal differences as the shear rate $\dot{\gamma}^\dagger$ increases. The lower graph shows $E*(\dot{\gamma}*)$, where $E*$ represents a hydrodynamic "temperature"; the kinetic energy increases steeply with shear-rate and large normal differences are manifested at low $\dot{\gamma}*$-shear rates. For $\dot{\gamma}* > 10$ the Stokesian flow curve is analytically predictable from the Newtonian viscosity of the thermal fluid; the scaling predicts ever-increasing apparent viscosity and dilatancy with increasing shear rate together with ever-decreasing relaxation and diffusion times.

at low shear-rate in the Stokesian flow curve. This arises because the effective friction coefficient is decreasing at a rate proportional $\dot{\gamma}^{\dagger 2}$ when $\eta^{\dagger}$ and y are constant.

The consequence of this preliminary observation is that the high shear-rate region of the isokinetic flow curve $\eta^{\dagger}(\dot{\gamma}^{\dagger})$ corresponds to the low shear-rate region of the mean-field Stokesian flow curve $\eta^{*}(\dot{\gamma}^{*})$ and vice-versa. In the Stokesian approximation, moreover, the high shear-rate region of the flow curve $\eta^{*}(\dot{\gamma}^{*})$, and other properties such as $D^{*}(\dot{\gamma}^{*})$, and $\mathbf{p}^{*}(\dot{\gamma}^{*})$, are analytically predictable from the Newtonian viscosity of the thermalised hard-sphere fluid, i.e. from $\eta^{\dagger}(\dot{\gamma}^{\dagger} \to 0, \mathrm{y})$, $D^{\dagger}$ and $\mathbf{p}^{\dagger}$ likewise.

The low shear-rate region of the isokinetic flow curve in the packing region of the fluid freezing transition is characterised by a disorder-order phase transition which stems from a shear perturbation of the equilibrium freezing transition for monodisperse spheres [11]. Assuming the inversion implied in equations (29)–(31) remains unaffected by the inclusion of many-body hydrodynamics or other perturbations, then the steady-state quasi-first-order transition corresponds to the well documented shear thickening disordering transition seen in dense suspensions at higher shear rates [26].

The osmotic pressure experienced at high shear in the $\dot{\gamma}^{*}$-flow curve is increasing as $\langle C^{\dagger} \rangle^{2}$ resulting in ever-increasing dilatancy in the high $\dot{\gamma}^{*}$-shear region. The osmotic pressure tensor scales as

$$\mathbf{p}^{*} = \mathbf{p}^{\dagger} E^{*} \left(\text{where } \mathrm{E}^{*} = \frac{\mathrm{E}^{\dagger}}{\mathrm{C}^{\dagger 2}} \right) \tag{33}$$

Figure 5 illustrates what happens, (i) to the coexistence pressure of the ordering transition and (ii) to the osmotic pressure (dilatancy) scales.

In the $\dot{\gamma}^{\dagger}$-flow curve both the kinetic energies and the diffusivities exhibit large normal differences with increasing shear rate; this leads to low perpendicular diffusivities, long relaxation times and glassy-like non-steady behaviour. The respective diffusion coefficients from soft-sphere data are shown in Figure 6. The diffusion coefficient scales as

$$D^{*} = D^{\dagger} E^{*1.2} \tag{34}$$

Figure 6 shows how the diffusivities exhibit large normal differences but these are expected to decrease with increased shear rate in the $\dot{\gamma}^{*}$-flow curve as the hydrodynamic system eventually maps on to the isotropic Newtonian thermalised system. The ever-increasing dilatancy, however, ensures that the hydrodynamic system at high shear rate can never be construed as Newtonian due to the ever-increasing "hydrodynamic temperature" at constant packing density. In all real geometries, i.e. conventional viscometers, concentration gradients and particle migrations from high-shear regions will eventually lead to inevitable instrumental artifacts and steady apparent viscosity which will vary with every device and its geometry.

At low shear rates in the $\dot{\gamma}^{*}$-flow curve we see that the osmotic contribution to the viscosity, pressure and the hydrodynamic diffusivity are decreasing and approach zero. This leads to ever-lengthening relaxation times rendering the steady-state laminar flow curve increasingly sensitive and dependent for measurement on laboratory time scales upon Brownian motion contributions to E*, D* and **p***. Brownian motion effects have not been explicitly incorporated into our computations yet. It seems likely that for higher y ($> \sim 40\%$) or larger shear rates (see next section) the effect is small, possibly negligible, but only by incorporating Brownian motion effects can we

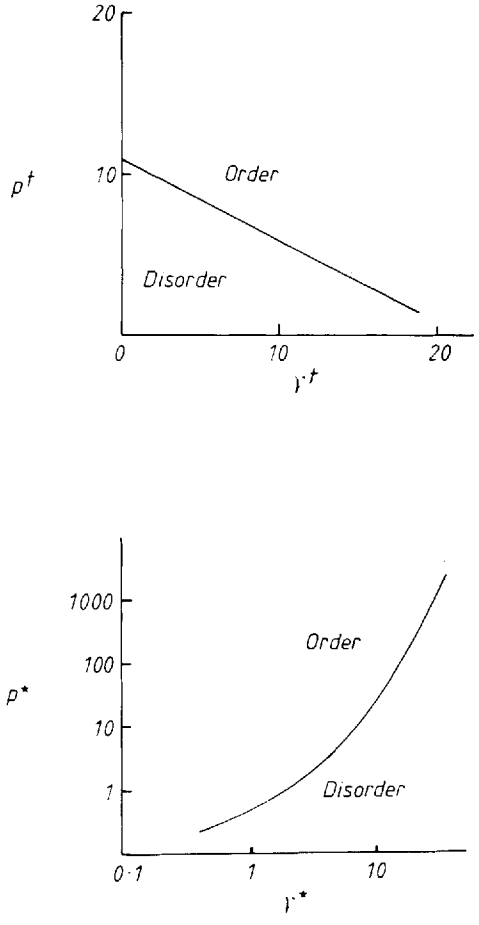

Figure 5 A prediction of the behaviour of the order-disorder transition for the hard-sphere model in the isokinetic flow form (upper graph) and mean-field Stokesian (lower graph); the linear and logarithmic axes, respectively, reflect the large increase in osmotic dilatancy in the hydrodynamic flow curve with increase in shear rate.

ensure a limiting Newtonian behaviour at low $\dot{\gamma}^*$. Even then the Brownian osmotic contributions may not be detectable on the ordinary laboratory measurement time scales.

In the hydrodynamic approximation the total stress in a sheared suspension can be resovled into two components. The hydrodynamic component, sometimes referred to as the intrinsic stress is, in the one-body mean-field approximation, the integral of the stress within the medium around the surface of a flowing sphere with stick conditions. The second component is the osmotic stress from the interparticle interactions. Therefore we can express the relative viscosity as the sum of the two components.

$$\frac{\eta}{\eta_m} = \left(1 + \frac{5}{2}y + \cdots\right) + 3\pi\eta^*. \tag{35}$$

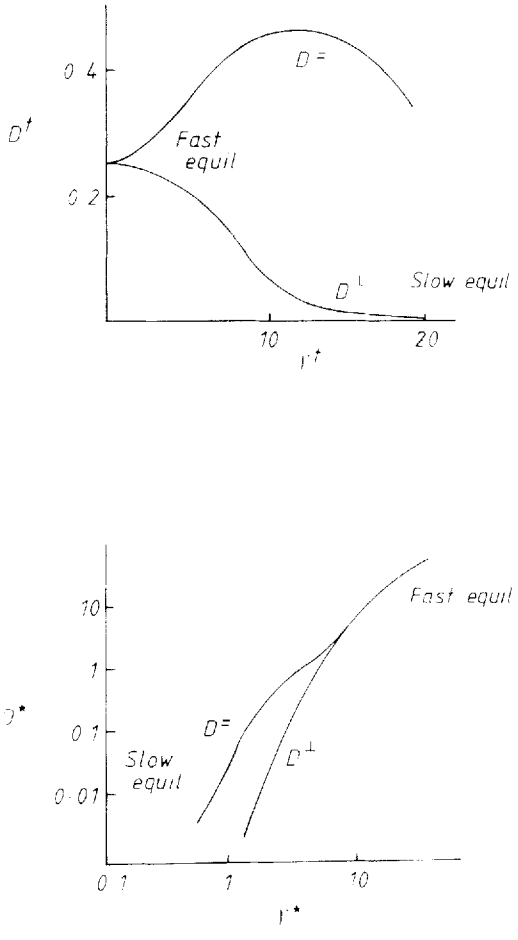

Figure 6 A comparison between the perpendicular ($D\perp$) and parallel (D'') diffusivities in the isokinetic and Stokesian mean-field flow curves; $D\perp$ is the mean of the unresolved D_{yy} and D_{zz} diffusivities for flow in the X-direction (these are close together compared to D_{xx}); the diffusivities determine the relaxation time for steady-state re-equilibration, thixotrophy and rheopexy, and particle migrations due to osmotic pressure gradients; the $\dot{\gamma}^*$-flow curve shows a strong increase in diffusivity with shear-rate which is analytically predictable from the equilibrium diffusivity of the thermal fluid.

Both the intrinsic hydrodynamic and osmotic contributions are generally shear-rate dependent but, neglecting many-body hydrodynamics, only the osmotic term is shear-dependent and this can be estimated from the hard-sphere scaling by the substitution $\eta^* = \eta^\dagger E^*(\dot{\gamma}^\dagger)$ giving

$$\frac{\eta}{\eta_m}(\dot{\gamma}^*) = 1 + \frac{5}{2}y + 3\pi\eta^\dagger E^* \tag{36}$$

Figure 7 shows the inversion of a soft-sphere flow curve from data in reference [21]. Without Brownian motion as $\dot{\gamma}^* \to 0$, the osmotic component goes to zero but the total apparent viscosity approaches the constant value given by the intrinsic contri-

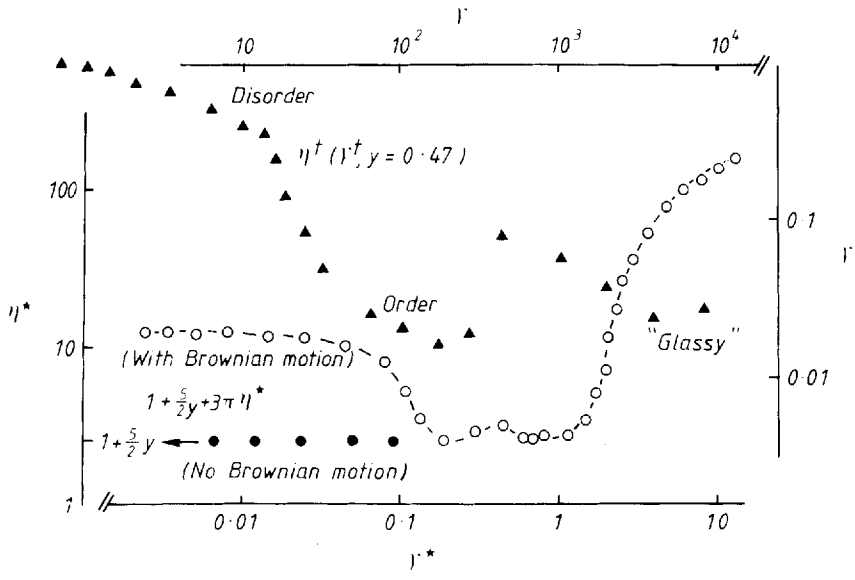

Figure 7 Data for a soft-sphere viscosity flow curve (from reference [21]) shown in both the isokinetic ($E_0 = \varepsilon$) and Stokesian forms; the 2-phase ordering transition to layered flow corresponds to the disordering shear thickening transition in the hydrodynamic $\dot{\gamma}$*-flow curve; without Brownian motion the viscosity is an ever-increasing function of $\dot{\gamma}$*-shear-rate over and above the hydrodynamic contribution; the effect of Brownian motion is to make steady-state equilibration possible at a low-shear rate on a certain time-scale which gives rise to time-dependent behaviour for the initial experimental shear thinning and the possibility of traversing the same transition twice; the high shear limiting behaviour is analytically predictable from the thermal equilibrium equation of state and viscosity behaviour.

bution. With increasing $\dot{\gamma}$*-shear rate the viscosity, as the dilatancy, is an ever-increasing function of the rate of shear. Dilatancy, osmotic pressure gradients, and particle migrations, in practice, ensure that the driving surface experiences a linear stress eventually in rheometric and engineering devices at high reduced shear rates.

6. BROWIAN MOTION

From the foregoing scaling arguments it is seen that the low-shear region of the $\dot{\gamma}$*-flow curve shows decreasing particle kinetic energies, diffusivities and osmotic stresses, all of which approach zero as $\dot{\gamma}$* approaches zero. On a fixed laboratory observation time scale, the experimental $\dot{\gamma}$*-flow curve must become time-dependent and non-steady as the relaxation times lengthen showing frozen in glass-like behaviour which does not correspond to the definition of a steady-state flow curve, i.e. a viscosity at zero frequency.

To define steady-state Newtonian behaviour in the low-shear region of the experimental flow curve thermal energy in the form of Brownian motion [28] must be present even though the steady-state manifestations of a thermal contribution may not be accessible or measurable on laboratory or engineering time scales for particles above the sub-micron size range. A number of authors have developed Brownian

dynamics for simulation of random motion by a superposition of the stochastic dynamics of random movements into the hydrodynamics [29–31]. Brownian motion effects have not yet been incorporated into our dynamical simulations of suspension rheology. As a precursor to such studies, however, we can examine the possibility of accommodating Brownian thermal motion into the scaling predictions by providing a base line steady-state for $E^*(\dot{\gamma}^*)$, $P^*(\dot{\gamma}^*)$ and $D^*(\dot{\gamma}^*)$ which ensures a limiting Newtonian behaviour at low $\dot{\gamma}^*$ and a continuous connection to thermodynamic equilibrium as $\dot{\gamma}^* \to 0$.

The conventional dimensionless group that is said to determine the importance of Brownian motion in sheared suspensions [28] is the Peclet ratio defined as

$$P_e = \frac{\dot{\gamma}\sigma^2}{D_o} \tag{37}$$

where D_o is the self-diffusion coefficient of an isolated particle and is related to the medium temperature and viscosity by the Stokes-Einstein relationship

$$D_o = \frac{kT}{3\pi\sigma\eta_m} \tag{38}$$

In order to get a qualitative feel for the effect of a low Peclet ratio on the steady state rheological flow curve $\eta^*(\dot{\gamma}^*)$ we can make a simple assumption. That is the scaling of $\eta^\dagger; p^\dagger; D^\dagger(\dot{\gamma}^\dagger)$ on to $\eta^*; p^*; D^*(\dot{\gamma}^*)$ depends only on $E^*(\dot{\gamma}^\dagger)$ in steady shear irrespective of the Brownian motion contribution of E^*. Thus, although there may be no unambiguous theoretical resolution of the kinetic energy of particles E^* contains a constant component which may be designated E_o^* which is independent of $\dot{\gamma}^*$.

Then

$$E^* = E_o^* + \frac{1}{C_{eff}^{\dagger 2}} \tag{39}$$

where $C_{eff}^\dagger$ is the time-average friction constant from an isokinetic simulation in which Brownian motion, prescribed by fixing the parameters in equation (38), is incorporated. The constant term E_o^* is a Brownian kinetic energy and may be written as

$$E_o^* = \frac{kT}{m\sigma^2 C^2} \tag{40}$$

and it represents the change in average relative separation of any two particles, i.e. $\Delta r_{ij}/\sigma$, in the characteristic hydrodynamic time C^{-1}.

Then

$$\dot{\gamma}^* = \dot{\gamma}^\dagger \left(E_o^* + \frac{1}{C_{eff}^{\dagger 2}} \right)^{1/2} \tag{41}$$

and

$$\frac{\eta}{\eta_m} = 1 + \frac{5}{2}y + 3\pi\eta^\dagger \left(E_o^* + \frac{1}{C_{eff}^{\dagger 2}} \right)^{1/2} \tag{42}$$

As the Peclet ratio $P_e \to 0$, $E_o^* \gg C_{eff}^{\dagger 2}$ and the Brownian energy dominates the scaling whereas at high $\dot{\gamma}^*$ (low $C^\dagger$) the Stokesian scaling is dominant. At low $\dot{\gamma}^*$ and low P_e

$$P_e \to 0, \qquad \frac{\eta}{\eta_m} = 1 + \frac{5}{2} + 3\pi\eta^{\dagger}\left(\frac{kT}{m\sigma^2 C^2}\right)^{1/2} \tag{43}$$

The effect of a Brownian motion contribution to a scaled soft-sphere $\dot{\gamma}^*$-flow curve is also shown in Figure 7 for the case when $E_0{}^*$ is given by equation (40). In the low P_e limit as $C \to 0$ we must also recover the Newtonian isokinetic scaling

$$\eta = \eta^{\dagger}\frac{(mkT)^{1/2}}{\sigma^2} \text{ and } \dot{\gamma} = \dot{\gamma}^{\dagger}\left(\frac{kT}{m\sigma^2}\right)^{1/2}$$

The scaled soft-sphere flow curve from equation (42) is compared in Figure 8 with a reduced flow curve from a recent experimental investigation of monodisperse silica spheres in cyclohexane [17]. Only the shear thinning region of the experimental flow curve can be seen through the laboratory 'window' in this case, but there is clearly a very large discrepancy with the scaling model predictions. More recent comparisons with the flow curves of larger 1–5 micron monodisperse suspensions also show a discrepancy in the same direction but reduced somewhat. The reason for this large discrepancy is presently unknown and could be due to one of several factors. An inspired guess is that the liquid medium is not behaving viscously in response to particle motions in the interstices between particles; the effective medium viscosity may be much larger than the bare value η_m of the pure liquid.

In this respect, the additional repulsive parameter in the colloidal sphere potential (equation (4)) could be parameterised to take account of the rôle of the solvation repulsion effect.

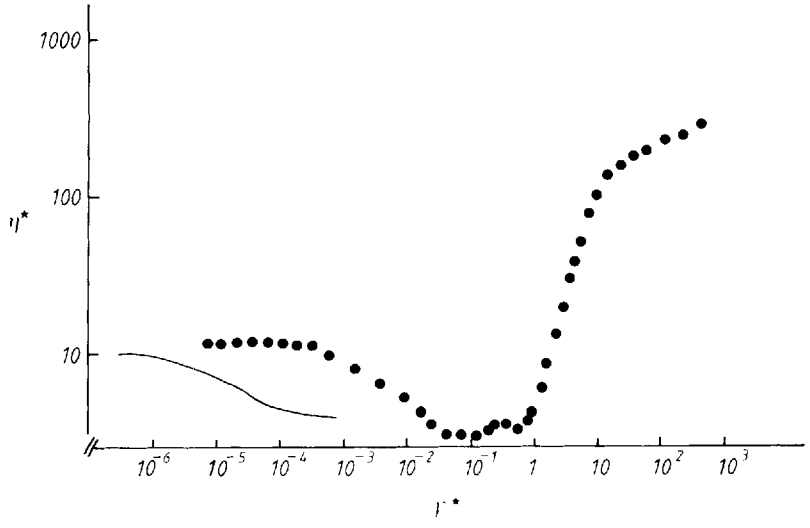

Figure 8 A comparison between the scaled $\dot{\gamma}*$-curve for the soft-sphere data (from reference [21]) and a reduced experimental flow curve for mondisperse silica spheres in cyclohexane taken from the work of de Kruijf et al. (reference [17]) at approximately the same effective packing; a very large discrepancy is seen on the reduced shear-rate scale but a reasonable prediction of the low shear viscosity is obtained when Brownian motion effects are roughly included.

7. GRANULAR DYNAMICS

The difficulties associated with the experimental rheological characterisation of dense colloidal suspensions at high shear rates become the predominant fetures of dry powder rheology. So complex are the effects of gravitational and shear induced pressure gradients, surface effects such as coulomb friction, polydispersity of size and shape, ill-defined system states etc., that virtually no progress has been made towards the prediction of the flow of powders in simple geometries, either under gravity or in pneumatic conveyance, from particulate parameters.

In the case of dry powders the dissipation of energy may be incorporated into dynamical simulations using the concept of the coefficient of restitution. This has been previously defined as the ratio of the final to initial relative velocities of two colliding particles. It varies from 0 form perfect inelasticity to 1 for completely elastic behaviour. A constant coefficient of restitution may be chosen for its simplicity and ease of application, for example to a colloidal-sphere potential. Experimental tests, however [32] indicate that the coefficient of restitution may be a complicated function of the initial impact velocity. Walton and co-workers [33] have reported computer simulation of the granular flow of two-dimensional inelastic discs using a velocity-dependent restitution coefficient.

By analogy with the previous investigations of the scaling laws for molecular fluids (section 3) and suspensions (section 4), however, it is anticipated that the constitutive rheology of a simple dry powder will be dominated by scaling, i.e. particle size, mass and granular "temperature", the detailed mechanisms of energy dissipation being a minor perturbation.

The simplest model of granular flow that retains both the essential physical effects and the scaling features corresponds to the homogeneous shear of inelastic, frictionless hard-spheres in a vacuum. In a steady state simulation the methods used previously [4,9] and outlined in section (3) for mean-field Stokesian dynamics, are then easily extended to granular dynamics by replacing the elastic collisions of classical conservative dynamics by inelastic collisions.

For an undamped simulation of the homogeneous shear of hard spheres, without a prescribed kinetic energy, the shear rate $\dot{\gamma}$ sets the time scale. If one performs an adiabatic simulation of sheared hard spheres the system heats up, as it heats up the stress decreases because the viscosity is temperature dependent; scaling shows this to be equivalent to an isothermal system with the shear rate decreasing with time. If all other properties are expressed in "isoshear" units (see table 2), the reduced constitutive rheology at steady state becomes Newtonian in the sense that the viscosity of the hard-sphere fluid must approach a unique material constant independent of the shear rate $\dot{\gamma}$ when expressed in reduced units (table 10. Alternatively, the shear rate and kinetic energy cannot vary independently; if they are forced to do so by fixing the kinetic energy whilst increasing the shear-rate a non-linear flow-curve eventually results when $\dot{\gamma}^{\dagger} > 1$ (approx.), accompanied by viscoelastic effects.

Non-Newtonian shear-dependent rheology is effected when the rate of shear is sufficient to distort the thermodynamic scaling, i.e. the total energy of the system is constrained relative to the characteristic energy $m\sigma^2\ \dot{\gamma}^2$to a degree such that the thermodynamic equilibrium is perturbed. Since experimental evidence indicates that for slight inelastic behaviour the coefficient of restitutuion is initially a linear function of the relative impact velocity [32], for the purposes of investigating the scaling laws

Table 2 Definitions of reduced properties and corresponding state scaling laws for granular dynamics; the basic units are particle mass (m), diameter (σ), restitution coefficient $\lambda = m\sigma/k$; k is defined in equation (44); g is the gravitational constant.

	Isoshear[(a)]	*Granular*	*Gravitational*
time	$t\# = t\dot{\gamma}$	$t^0 = t\lambda$	$\tilde{t} = t(g/\sigma)^{1/2}$
kinetic energy (granular "temperature")	$E\# = \frac{E}{m\sigma^2\dot{\gamma}^2}$	$E^0 = \frac{E}{m\sigma^2\lambda^2}$	$\tilde{E} = \frac{E}{gm\sigma}$
velocity	$v\# = \frac{v}{\dot{\gamma}\sigma}$	$v^0 = \frac{v\lambda}{\sigma}$	$\tilde{v} = \frac{v}{g\sigma}$
strain rate (tensor)		$\dot{\gamma}^0 = \dot{\gamma}/\lambda = \frac{\dot{\gamma}^\dagger}{\lambda^\dagger}$	$\tilde{\dot{\gamma}} = \dot{\gamma}(\sigma/g)^{1/2}$
restitution coefficient	$\lambda\# = \lambda/\dot{\gamma}$	$(\lambda = m\sigma/k)$	$\tilde{\lambda} = \lambda(\sigma/g)^{1/2}$
pressure (tensor)	$\mathbf{p}\# = \mathbf{p}\frac{\sigma}{m\dot{\gamma}^2}$	$\mathbf{p}^0 = \frac{\mathbf{p}\sigma}{m\lambda^2} = \frac{\mathbf{p}^\dagger}{\lambda^{\dagger 2}}$	$\tilde{\mathbf{p}} = \mathbf{p}\frac{\sigma^2}{gm}$
viscosity[(b)]	$\eta\# = \eta\frac{\sigma}{m\dot{\gamma}}$	$\eta^0 = \frac{\eta\sigma}{m\lambda} = \frac{\eta^\dagger}{\lambda^\dagger}$	$\tilde{\eta} = \frac{\eta\sigma^{1/2}}{mg^{1/2}}$
diffusivity	$D\# = \frac{D}{\dot{\gamma}\sigma^2}$	$D^0 = \frac{D}{\lambda\sigma^2} = \frac{D^\dagger}{\lambda^\dagger}$	$\tilde{D} = \frac{D}{(g\sigma^3)^{1/2}}$

(a) the isoshear properties correspond to the isokinetic reduced properties (table 1) by the substitution for $\dot{\gamma} = \dot{\gamma}^\dagger(E_0/m\sigma^2)^{1/2}$.
(b) the viscosity in the isoshear scheme is the same quantity as the reduced stress ($p_{xy}^\#$); in granular flow a simple steady-shear viscosity as we ordinarily define it may not be relevant, in general the rheology is described as a deformation rate-dependent fourth-rank tensor, but the isoshear scaling shows that it will map on to an isokinetic hard-sphere state point when the granular "temperature" is high.

we can redefine a coefficient of restitution by analogy with the definitions of the mean Stokes friction constant in section (4).

To investigate the scaling of steady-state homogeneous shear rapid granular flow of slighly inelastic spheres the coefficient of restitution may be defined as a material constant, i.e. as the constant of proportionality between the relative energy loss and the impact speed; then the restitution coefficient is $(1 - k\mathbf{v}_0)$ and

$$\Delta E = k\mathbf{v}_0^3 \tag{44}$$

E_{ij}^0 is the initial kinetic energy of the colliding pair and by analogy with the definition of the Stokes constant C it is convenient to redefine a characteristic frequency $\lambda = m\sigma/k$ which sets the time scale; the determination of its mean value from isokinetic NEMD leads to the corresponding state predictions for rapid granular flow (table 2).

For hard-sphere granular dynamics the particle velocities between the collisions are constant and the algorithm for the change in velocity on collision of two inelastic spheres is

$$\mathbf{v}_i(\text{new}) = \mathbf{v}_i(\text{old}) + \frac{b_{ij}\mathbf{r}_{ij}}{\sigma^2}\left[1 - \frac{\mathbf{v}_{ij}\sigma}{2\lambda}\right] \tag{45}$$

where $b_{ij} = \mathbf{r}_{ij}\mathbf{v}_{ij}$

An energy balance shows that the rate of energy dissipation and rate of viscous heat production at steady state is then

$$\frac{Nvk\langle \mathbf{v}_o^3 \rangle}{4} = \eta\dot{\gamma}^2 V \tag{46}$$

where v is the collision frequency of a sphere.
From the equation-of-state the collision frequency is exactly given by

$$v^\dagger = \left(\frac{p}{\varrho kT} - 1\right)\left(\frac{9}{\pi}\right)^{1/2} \tag{47}$$

in isokinetic units; the isokinetic-reduced mean restitution coefficient can therefore be calculated from isokinetic hard-sphere steady-shear rheology

$$\langle \varepsilon^\dagger \rangle = \frac{9\varrho(z-1)}{\eta^\dagger \dot{\gamma}^{\dagger 2}} \tag{48}$$

where $z = p/\varrho kT$.

Again, it is seen that the Newtonian viscosity of the thermalised hard-sphere fluid at low $\dot{\gamma}^\dagger$-shear can be used to predict the flow curve for rapid granular flow from $E^0(\dot{\gamma},y)$ where the granular temperature E^0 is given by

$$E^0 = \frac{E^\dagger}{\dot{\gamma}^{\dagger 2}} \tag{49}$$

Scaling laws for the other quantities, for example, stress and isotropic pressure, are given in table 2. Thus, we see that the rapid granular flow domain is analytically predictable from the invariant "isoshear" Newtonian viscosity of the dense hard-sphere fluid (table 2). The behaviour of dry powders at high rates of shear corresponds to the highly non-Newtonian, high $\dot{\gamma}^\dagger$-shear region of the isokinetic flow curve in the high packing - low energy range in this limiting form.

In typical laboratory experiments of granular flow, for example gravitational flow down a chute, the stress is fixed and the velocity and/or velocity gradients are monitored. In these cases it is both convenient and instructive to work with an alternative set of scaling units in terms of the gravitational constant g (table 2) which determines the prescribed stress.

We have begun to carry out simulations using these schemes for three-dimensional hard spheres and colloidal spheres [34]. Some preliminary results for the velocity profile from a simulation of colloidal spheres using a constant coefficient of restitution are shown in Figure 9. This inhomogeneous flow system has a free boundary with the bottom layer of particles "stuck" on the surface of the chute. The initial results for a 500 particle system, periodic in the two perpendicular directions, do not show a region with a linear velocity profile but show significant surface effects and substantial dilatancy with granular "temperature".

The foremost objective in predicting powder flow is to characterise the regions of flow, e.g. types A, B, C, D in the Geldart classification [35] using the scaling variables we have introduced. The low $\tilde{\gamma}$-shear region clearly corresponds to something approaching plug flow, low particle kinetic energies and time-dependent yield stresses, and the high-shear region represents isotropic (easily aeratable?) rapid flow. The cohesive class type C corresponds to the low $\tilde{\gamma}$ shear region when the characteristic attractive pair energy (ε) due to absorbed layer bridging is much greater than $gm\sigma$ and the flow is in the low $\tilde{\gamma}$ shear region. Work is presently in progress to determine the characteristic yield and fracture stresses of these scaleable models to identify the scaling regions with the diversity of experimental behaviour.

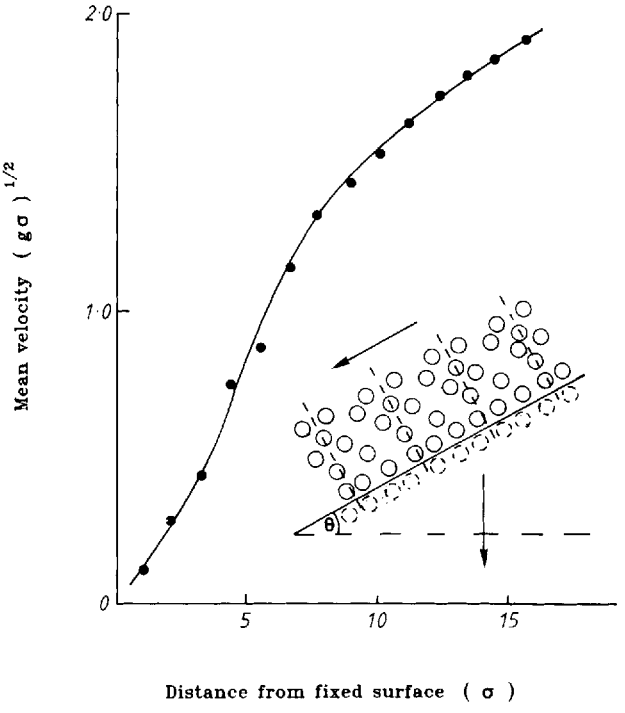

Figure 9 Preliminary results for the steady gravitational flow of colloidal soft-spheres down a chute from a simulation of 512 spheres with periodic boundary conditions in two of the three dimensions perpendicular to the flow direction; the velocity profile does not show a linear region and is steeper in the region of the rigid granular surface of the chute (reproduced from reference [34]).

8. CONCLUSIONS

This present approach towards the prediction of complex constitutive rheology for colloidal suspensions and dry powders is based upon a simple premise; the rheology of a particulate system at high concentration, from molecules to granules or globules in suspension, can be resolved into a scaleable component and perturbations. The scaleable component determines the time-scale for behaviour as seen through the laboratory experimental "window", and depends only upon the particle mass, size and characteristic time/frequency or kinetic energy scale. The second component represents hitherto unknown effects which may be perturbations due to non-scaleable terms in the interparticle forces, e.g. non-sphericity, non-pairwise additivity, polydispersity of shape and size, or in the equaitons of motion, e.g. many-body hydrodynamic or solvation effects. At this stage, it would not be sensible to attempt to incorporate these complexities directly into the simulations of specific fluids until the properties of the scaleable core models have been fully computed, understood, and evaluated for inadequacies against available experimental data.

The alternative approach of dressing up an effective pair potential with empirical parameters, to the best of our presently limited knowledge, and simultaneously including complex terms in the equations-of-motion would, at this stage yield results which were of little theoretical or practical value, even if both the input parameters

and computer power were available. Indeed, although substantial technical progress has recently been made in the simultaneous incorporation of Brownian motion and many-body hydrodynamics [31], results reported so far are restricted to tens of particles in two-dimensions in the low Reynolds number limit, and are still far removed from the rheology of dense colloidal suspensions.

The most significant conclusion to emerge from the scaling analysis of the hard-sphere fluid Newtonian viscosity and its isokinetic flow curve, is that it is essentially the same as the constitutive rheology of Stokesian spheres in the mean-field approximation, and it is also the same as the rheology of inelastic frictionless spheres, the variations with the material constants C or λ and the particle parameters m and σ being entirely analytically predictable from the isokinetic hard-spheres fluid. The need now is to accurately determine the flow curves over the whole range of packing density for the hard- and, more generally, colloidal-sphere models, in any one of the isokinetic, Stokesian or granular forms so that we can map on to experiment.

Early indications are that the continuous hydrodynamic concept is inapplicable for denser suspensions of fine particles and that the solvation effects dominate the close-contact dynamics. The bare medium viscosity is not an appropriate material constant for the scaling although it may be used in conjunction with an empirical effective colloidal-sphere potential. It appears that thermodynamic osmotic equation-of-state, i.e. osmotic pressure data, at higher concentrations will be invaluable in the determination of the effective pair potential parameters appropriate to the rheology and its prediction from the scaling laws; the osmotic deformation moduli should determine effective C and λ values.

On the experimental side, the scaling laws clearly highlight the well-known difficulties encountered in trying to measure a unique steady-state flow curve for a granular suspension as we ordinarily define it. The analytic scaling laws alone show that the effect of a shear field is to drastically, and continuously, with increasing shear rate, change the quasi-thermodynamic (osmotic) state of the system by increasing the osmotic pressure. The scaling laws further show that at low reduced shear rates the non-Newtonian rheology of the isokinetic high-shear region manifests itself showing extreme time-dependent and anisotropic behaviour. At high shear-rates the hydrodynamic and granular flow curves are analytically predictable from the hard-sphere "isoshear" fluid Newtonian viscosity *but* the experimental systems cannot be construed as Newtonian since the scaling predicts ever-increasing viscosity and dilatancy with shear-rate, coupled to ever-decreasing relaxation time due to the enhanced kinetic energies of the particles. These combined effects make both the low shear (in the absence of sufficient Brownian motion), and the high shear steady-state flow curve at constant concentration virtually impossible to measure with present conventional rheometric devices.

Acknowledgement

This research work is financed by the SERC and is carried out under the auspices of the Specially Promoted Programme in Particulate Technology; it is also supported by the International Fine Particle Research Institute (IFPRI). In both respects I wish to thank Mr. L.J. Ford for advice and encouragement, and to acknowledge many helpful discussions with colleagues M.F. Edwards, H.A. Barnes, D. Geldart, A.I. Jomha, A.J. Hopkins and M.C. Turner.

APPENDIX I

Equilibrium osmotic pressure data (pV/NkT) for the colloidal-sphere model $\phi = \varepsilon(r/\sigma - 1)^{-n}$ for n = 12 from MD computations (N = 500) (maximum statistical uncertainty is ~ 5%)

density (ϱ) ($kT/\varepsilon = 10^{12}$)	*fluid*	*crystal (fcc)*	*kinetic energy (kT/ε) ($\varrho = 0.8$)*	
0.1	1.35		10^{12}	26.90
0.2	1.81		10^{12}	26.90
0.3	2.56		10^{16}	11.45
0.4	3.66		10^{18}	10.02
0.5	5.30		10^{20}	8.87
0.6	8.02		10^{22}	8.25
0.7	12.54	10.17(a)	10^{24}	8.18
0.8	26.90	12.40	10^{26}	7.99
0.9	291.8(a)	23.41	10^{28}	7.75
1.0		64.35	∞	7.50

(a) these are metastable states: the coexistence pressure is at present unknown.

APPENDIX II

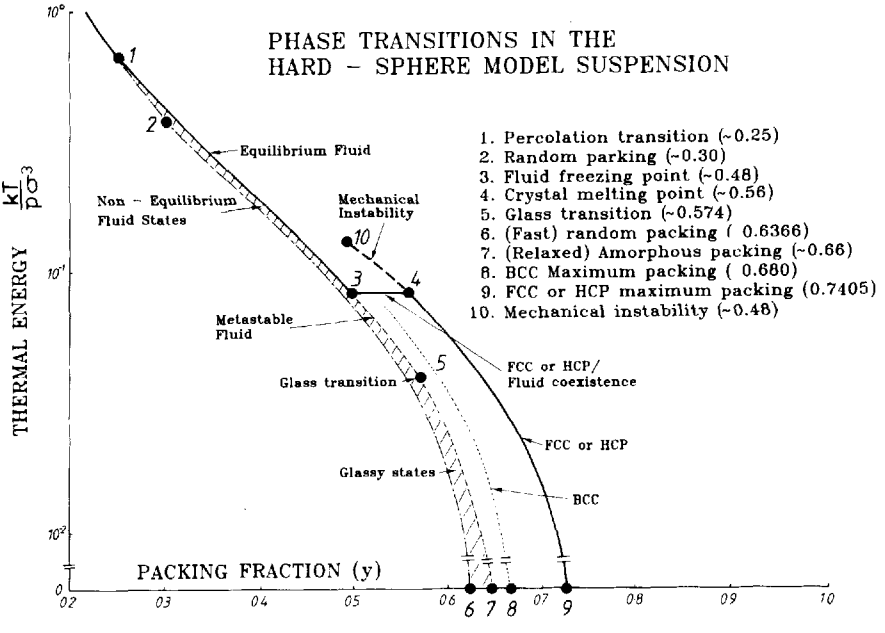

Figure 10 A schematic picture of the equilibrium, metastable equilibrium and relevant non-equilibrium static phase behaviour of the hard-sphere model; reproduced from report to SERC (by A.I. Jomha and L.V. Woodcock) specially promoted programme in particulate technology (1988).

APPENDIX III

When a model suspension is simulated with Lees-Edwards boundary conditions [6] and a uniform flow field ($\dot{\gamma}$) is imposed on the velocities the equations-of-motion (14 and 15) take the form

$$d\mathbf{r}_i = (\mathbf{v}_i + d\mathbf{v}_x^0)\, dt$$

$$d\mathbf{v}_i = \frac{1}{m}(\mathbf{F}_i^{(H)} + \mathbf{F}_i^{(P)})\, dt$$

Whereupon

$$\frac{d\mathbf{v}_x^0}{dt} = \frac{d\mathbf{v}_x^0}{dY_i}\frac{dY_i}{dt} = \dot{\gamma}\mathbf{v}_y$$

and the time to the next collision for hard-spheres can be calculated from the following quartic equation by taking the smallest positive real root

$$\begin{aligned} r_{ij}^2 - \sigma^2 + 2[\mathbf{r}_{ij}(0)\,\mathbf{v}_{ij}(0) + X(0)\,\dot{\gamma}Y(0) + \mathbf{v}_x(0)X(0)]\,t^* \\ + [v_{ij}^2 + \dot{\gamma}X(0)\,v_y(0) + \dot{\gamma}^2\,Y(0)^2]\,t^{*2} \\ + [Y(0)\,\dot{\gamma}^2\mathbf{v}_y(0) + \mathbf{v}_x(0)\,\dot{\gamma}\mathbf{v}_y(0)]t^{*3} \\ + [1^4\,\dot{\gamma}^2v_y^2(0)]\,t^{*4} = 0 \end{aligned}$$

where $t^* = [1 - \exp(-Ct)]/C$

References

[1] H.J.M. Hanley, D.J. Evans, S. Hess, W.G. Hoover, B.J. Alder, W.E. Alley, R.B. Bird and C.F. Curtiss, "Fluids out of equilibrium", *Physics Today* **37**,25 40 (January 1984).

[2] R. Zwanzig, "Time-correlation functions and transport coefficients in statistical mechanics", *Ann. Rev. Phys. Chem.* **16,** 67 (1965).

[3] M.P. Allen and D.J. Tildesley, "The computer simulation of liquids", Clarendon press, Oxford; 1987).

[4] B.J. Alder, D.M. Gass and T.W. Wainwright, "Studies in molecular dynamics VIII: the transport coefficients for a hard-sphere fluid", *J. Chem. Phys.* **53,** 3813 (1970).

[5] D. Levesque, L. Verlet and J. Kurkijarvi, "Computer experiments on classical fluids IV: transport properties and time correlation functions of the Lennard-Jones system near its triple point", *Phys. Rev.* **A7,** 1690 (1973).

[6] A.W. Lees and S.F. Edwards, "The computer study of transport processes under extreme conditions", *J. Phys. (C)* **5,** 1921 (1972).

[7] E.M. Gosling, I.R. McDonald and K. Singer, "On the calculation by molecular dynamics of the shear viscosity of a simple fluid", *Mol. Phys.* **26,** 1475 (1973).

[8] W.T. Ashurst and W.G. Hoover, "Dense fluid shear viscosity via non-equilibrium molecular dynamics", *Phys. Rev.* **All,** 658 (1975).

[9] T. Naitoh and S. Ono, "The shear viscosity of a hard-sphere fluid via non-equilibrium molecular dynamics", *J. Chem. Phys.* **70,** 4515 (1979).

[10] L.V. Woodcock, "Origins of shear dilatancy and shear thickening phenomena", *Chem. Phys. Let.* **111,** 455 (1984).

[11] L.V. Woodcock, "Origins of thixotropy", *Phys. Rev. Lett.* **54,** 1513 (1985).

[12] H.A. Barnes, M.F. Edwards and L.V. Woodcock, "Applicaitons of computer simulations to dense suspension rheology", *Chemical Engineering Science* **42** 591 (1987).

[13] W.T. Ashurst and W.G. Hoover, "Dense fluid shear viscosity and thermal conductivity – the excess", *A.I. Chem. E. Journal* **21,** 410 (1975).

[14] L.V. Woodcock, "Computer simulation of molecular liquids", Chapter 14 in "Organic Liquids" Eds. Buckingham, Lippert and Bratos, (John Wiley and Co.: London 1978).
[15] E.J.W. Verwey and J.Th.G. Overbeck, "Theory of the stability of lyophobic colloids", (Elsevier: Amsterdam 1948).
[16] L.V. Woodcock, "Glass transition in the hard-sphere model and Kauzmann's paradox", *Annals New York Acad. Sci.***371,** 274 (1981).
[17] C.J. de Kruijf, E.M.F. van Iersel, A. Vrij and W.B. Russel, "Hard sphere colloidal dispersions: viscosity as a function of shear rate and volume fraction", *J. Chem. Phys.* **83,**4717 (1985).
[18] S. Bell, "Soft-sphere viscosity predictions", Dissertation, School of Chemical Engineering, University of Bradford (1986) (unpublished results available from the author).
[19] J.O. Hirchfelder, C.F. Curtiss and R.B. Bird, "Molecular theory of gases and liquids", Appendix 1A p.1110 (John Wiley & Sons Inc.: New York 1954).
[20] P.J. Millard, "Soft-sphere thermal conductivity predictions", Dissertation, School of Chemical Engineering, University of Bradford (1987) (unpublished results available from the author).
[21] D.M. Heyes, "Non-Newtonian behaviour of simple liquids", *J. Non-Newtonian Fluid Mech.* **21,** 137 (1986).
[22] L.V. Woodcock, "Some *ad hoc* notes on isokinetic and NVT dynamics", *SERC-CCP5 Quarterly Newsletter for the Computer Simulation of Condensed Phases* **24,** 29 (Daresbury Laboratory U.K.; March 1987).
[23] D.J. Evans and G.P. Morriss, "Non-Newtonian molecular dynamics", *Computer Physics Reports* **1,** 297 (1984).
[24] L.V. Woodcock, "Mean-field Stokesian dynamics", SERC-CCP5 Quarterly Newsletter for the Computer Simulation of Condensed Phases (Daresbury Laboratory, U.K.; December 1987).
[25] H.J.C. Berendsen, J.P.M. Postma, W.F. van Gunsteren, A. Di Nola and J.R. Hask, "Molecular dynamics with coupling to an external bath", *J. Chem. Phys.* **81,**3684 (1984).
[26] H.A. Barnes, "Shear-thickening ("dilatancy") in suspensions of non-aggregating solid particles dispersed in Newtonian liquids: a review and practical guide", in press.
[27] C.E. Chaffey, "Mechanisms and equations for shear thinning and shear thickening in dispersions", *Colloid and Polymer Science* **225,** 691 (1977).
[28] W.B. Russel, "Brownian motion of small particles suspended in liquids", *Ann. Rev. Fluid Mech.* **13,** 425 (1981).
[29] D.L. Ermak and J.A. McCammon, "Brownian dynamics with hydrodynamic interactions", *J. Chem. Phys.* **69,** 1352 (1978).
[30] J. Bacon, E. Dickinson and R. Parker, "Simulation of particle motion and stability in concentration dispersions", *Faraday Disc. Chem. Soc.* **76,** 165 (1983).
[31] G. Bossis and J.F. Brady, "Self-diffusion of Brownian particles in concentrated suspensions under shear"**87,** 5437 (1987).
[32] W. Goldsmith, "Impact: the theory and physical behaviour of collidings solids", (Edward Arnold: London 1960).
[33] O.R. Walton and R.L. Braun, "Viscosity, granular-temperature and stress calculations for shearing assemblies of inelastic, frictional disks", *Journal of Rheology* **30,** 349 (1986).
[34] D. Geldart, M.C. Turner and L.V. Woodcock, "Characterisation and prediction of powder flow", International Fine Particle Research Institute (IFPRI) Annual Report (1987).
[35] D. Geldart, "Types of gas fluidisation behaviour", *Powder Technology* **7,** 285 (1973).